The Electrostatic Joint Space

Computer Integrated Surgery II

Project Proposal

Student: Qian Cao

Mentor: Prof. Jeffrey Siewerdsen

I. Project Summary

Normal anatomical variations in knee morphology can function as potent predictors of risk-of-injury when the body is under stress, such as in weight-bearing conditions [1-6]. With the recent development of a dedicated extremity cone-beam computed tomography (CBCT) scanner at Hopkins [7], CT volumes can now be acquired when the subject is standing in a load-bearing state. This combination of high image quality and new configuration provides an opportunity to investigate the relationship between risk-of-injury under load-bearing conditions and features of knee morphology. However, conventional methods of analyzing knee morphology is lacking in consistency and accuracy. In this project, a novel method of characterizing the joint space in the knee will be developed and validated.

II. Background and Specific Aims

Knee morphology has long been used to reveal severity of pathologies such as rheumatoid arthritis, gout and a variety of other diseases. Various methods of assessing the morphology co-exist, each popular within their own modalities and tailored to specific pathologies. In radiographs, a long standing (and evolving) tradition is the Sharp-Larsen Score [8]; in MRI, the gold standard for diagnosing rheumatoid arthritis is the rheumatoid arthritis MRI scoring (RAMRIS) system [9]. Though these methods measure common features such as joint space narrowing and cartilage thinning, they are highly qualitative and/or difficult to reproduce consistently. For example, the Sharp-Larsen score is extremely difficult to standardize, as beam direction, knee position, foot rotation are all variables affecting the final result. Along with RAMRIS, the Sharp-Larsen method also utilizes a simple scoring system based on qualitative descriptions to classify the patient's condition into only a few categories.

In recent years, studies have proposed quantitative methods for assessing the joint space in CT volumes of the knee [10], including projection along a longitudinal axis and the closest point algorithm. In the former method, lines are projected from one surface to the other along a predefined axis (Figure 1), the lengths of these lines are then measured and defined to be the distance between the two surfaces. This method, though straightforward, is difficult to implement in a practical situation, as it is somewhat arbitrary what the predefined axis should be, especially taking into account the complex geometry of the femur and tibia. Moreover, the configuration of the patient (whether she is standing or sitting) also influences the selection of the predefined axis.

Selecting the “right” axis is not just hard but also has significant impact on the result, as shown in figure 1 c) and d), a slight deviation of the axis can produce a drastically different distance map between two surfaces.

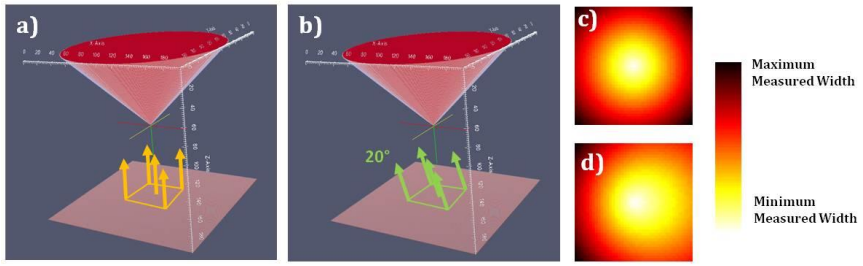

Figure 1 A simple example of measurements with the projection along a longitudinal axis method. In a) the predefined axis is parallel to the z-axis, producing a mapping c) of measured distance between the plane and cone. In b) the predefined axis is tilted by 20 degrees, producing a mapping d).

The latter method evades some of the aforementioned problems. The closest point algorithm calculates for each point on a surface, the distance to its closest point on the other surface. This method is slightly more sophisticated, but not problem-free. For example, figure 2 shows the same cone-plane geometry as depicted in figure 1, when mapping from the cone to the plane (figure 2b), each point on the surface of the cone maps vertically down onto the plane, producing the same distance map as did figure 1a. However, when mapping from the plane to cone (figure 2a), the tip of the cone is the closest point to every point in the region of interest on the plane. Thus the mappings are completely different. This could be a problem when handling sharp protrusions on either surface. As with the case in figure 2a, the full 3D volume information (the majority of the surface area on the cone) is not taken into account.

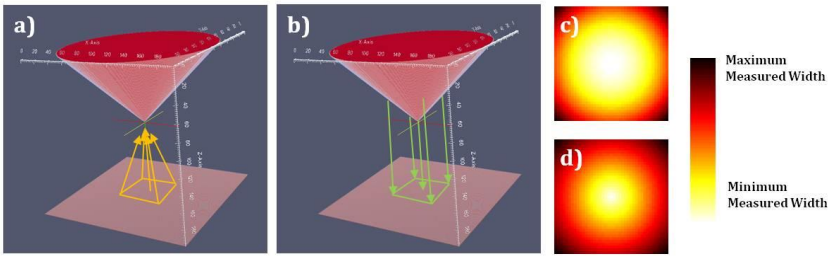

Figure 2 A simple example of measurements with the closest point method. In a) the mapping is constructed from the square region on the plane to the cone. In b) the mapping is constructed from the surface of the cone to the plane.

The two methods described above are based on rather artificially defined distance functions. In this project we derive a more elegant solution (originally proposed in [7]) from the laws of physics, in the form of Maxwell’s equations. If we consider the two surfaces to be the terminals of a capacitor differing in electric potential, a gradient of electric potential will exist between them. By tracing the gradient, we obtain the electric field lines from one surface to the other (figure 3). These lines are

perfectly bijective, independent of any arbitrary selection of axes, continuously distributed across both surfaces and unique to the geometry of the space.

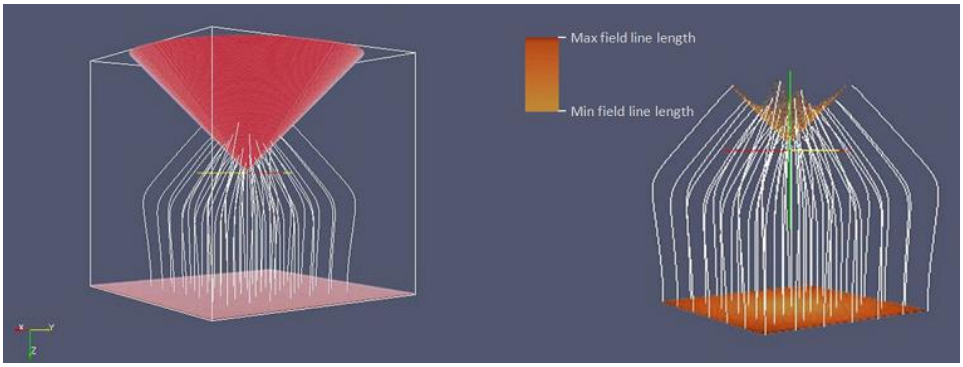

Figure 3 The distance between the cone and plane mapped with electric field lines derived from the capacitor model. In the right subfigure, the region of interest is colormapped so that the smaller distances correspond to lighter color. Figures were created as part of the preliminary findings described in the next section.

The specific aims of the project are to:

1. Implement an algorithm that generates a joint space map (JSM) based on the capacitor model.
2. Validate and test the algorithm on real knee volume data.
3. Provide thorough documentation and analysis of the algorithm for future biomechanical studies.

III. Technical Summary of Approach and Preliminary Findings

Joint Space Mapping

At the heart of the algorithm is the need to accurately compute the distribution of the electric potential in the joint space. Consider Gauss's law for electric fields in differential form:

$$\nabla \cdot \vec{\mathbf{E}} = \frac{\rho}{\varepsilon_0} \qquad (1)$$

where ρ is the charge density [C/m^3] and ε_0 is the electric permittivity of free space [C/(Vm)].

According definition, the electric field is the gradient of the potential:

$$\vec{\mathbf{E}} = -\nabla\Phi \qquad (2)$$

By substitution of (2) into (1), we obtain:

$$\nabla^2\Phi = -\frac{\rho}{\varepsilon_0} \qquad (3)$$

To solve for Φ, we assume $\forall\, x \in R$, $\rho(x)=0$, in which case equation (3) becomes the Laplace equation $\nabla^2\Phi=0$ with boundary conditions: $\Phi(\partial_0 R)= +V$ and $\Phi(\partial_1 R)= -V$ (figure 4a).

The Laplace equation can then be solved numerically using the finite difference method, specifically the widely-known method of relaxation. This can be used because the solution to a Laplace equation is a harmonic function and a point in such a function is the average of its surrounding points. In our method of relaxation, an iterative procedure in which each point is set to the average of its neighbors is applied to the volume [11]. Specifics of the approach as well as augmentations for enhanced speed and accuracy is still in development. Once the potential field is obtained, the volume as well as the electric field (gradient of the potential) can be interpolated and electric field lines can be computed by stepping from one surface to another.

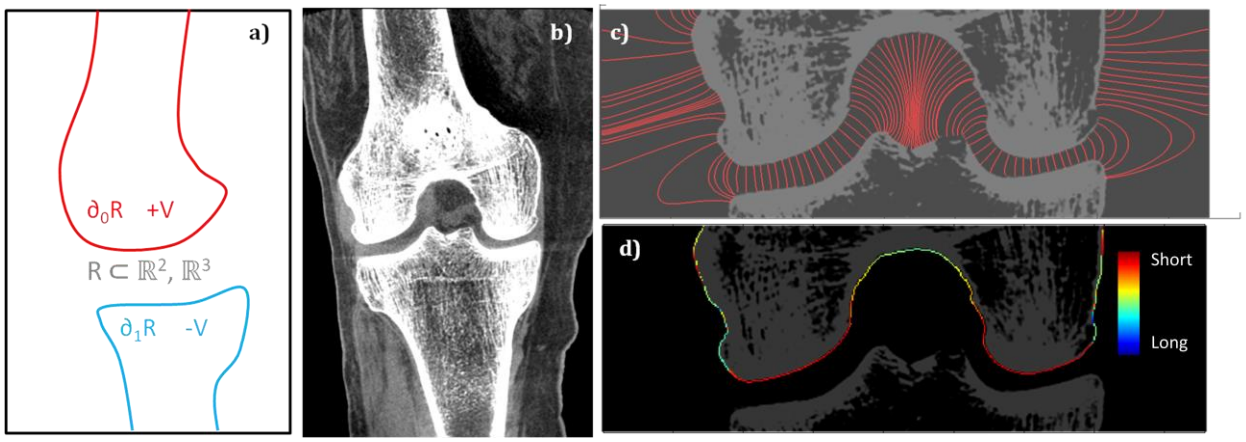

Figure 4 a) Problem formulation: the capacitor model. b) A realistic coronal CT slice of a knee (Courtesy of Prof. Siewerdsen) c) Computed electric field lines in 2 dimensions. d) A mapping of field line lengths of lines originating from the femur. Warm colors correspond to origins of short field lines and cold colors long ones.

The preliminary analysis in figure 4 showcases the approach in two dimensions. In three dimensions, we would obtain 3D mappings of the joint space width as two surfaces: the surfaces of femur and tibia.

GPU Acceleration

The averaging procedure used in the method of relaxation can be formulated as a multidimensional convolution with a special averaging mask. This is significant because convolution is very easy to parallelize with existing libraries on a GPU. Preliminary benchmarks have revealed that the computation of the field potential can be accelerated up to 50 fold in the size regime of the existing test CT volumes. Though the code has yet to be profiled and further optimized, it does gives me confidence that a performance boost would be obtained in parallelizing the procedure.

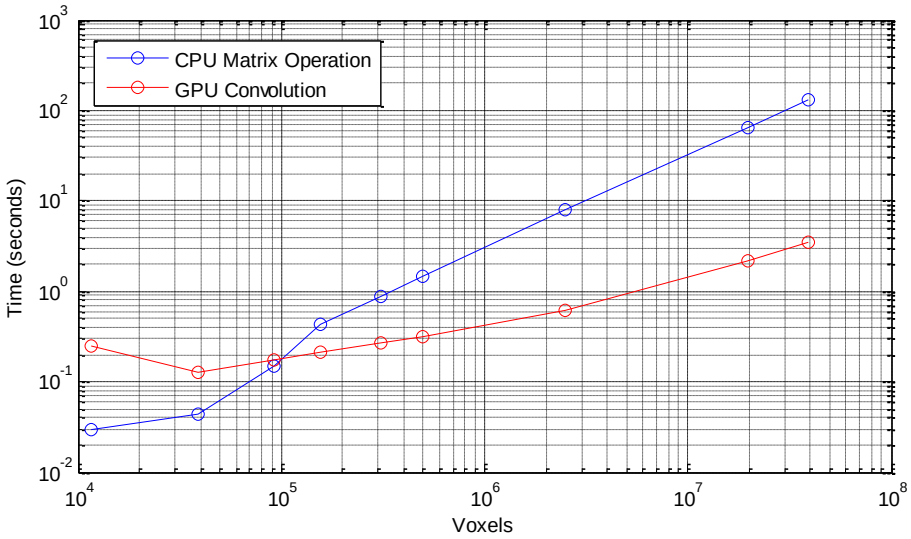

Figure 5. Benchmark comparing the time to complete 10 iterations on the same volume for GPU and CPU implementation

Segmentation of the Femur and Tibia

Segmentation is a critical piece of the algorithm because the quality of the potential distribution within the joint space depends heavily on the quality of the segmentation data, though the details remain to be worked out.

IV. Deliverables

Minimum Deliverable (Expected by 03/01/2014)

1. A set of prototyped MATLAB functions for joint space analysis using the capacitor model.
2. A set of prototyped MATLAB functions for segmentation.

Expected Deliverable (Expected by 04/01/2014)

1. A set of validated and refined MATLAB functions for joint space analysis using the capacitor model.
2. A refined MATLAB function for segmentation.
3. Detailed analysis of algorithm performance (convergence characteristics, accuracy, speed etc)

Maximum Deliverable (Expected by 05/01/2014)

1. MATLAB routines for visualization of the analysis results (volume rendering + GUI) in VTK and QT.
2. Detailed in-line and PDF documentation of all code.

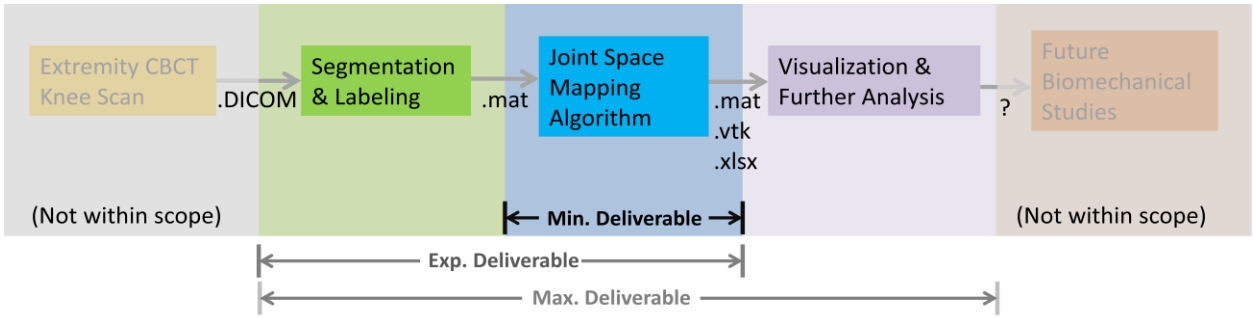

Figure 6 Overview of project scope and the hierarchy of deliverables within the pipeline of the main study. Possible interfaces (file formats) between various parts of the pipeline is also denoted.

V. Schedule and Milestones

Stage	Task	6-Jan	13-Jan	20-Jan	27-Jan	3-Feb	10-Feb	17-Feb	24-Feb	27-Feb	3-Mar	10-Mar	17-Mar	24-Mar	31-Mar	7-Apr	14-Apr	9-May
Preliminary Experimentation	Literature Review																	
	Problem Formulation																	
	Method Selection																	
	Synthesize Toy Data																	
	Experiment with Methods for Knee Volume Segmentation																	
	Prototype Algorithm for Joint Space Analysis																	
	Experiment with Visualization Toolchain (Volume Rendering, etc)																	
	Preliminary Profile and Benchmark																	
	Project Proposal Presentation																	
	Milestone #1																	
Algorithm Validation and Refinement	Refine and Test Segmentation Method																	
	Apply Joint Space Analysis Algorithm to Knee Data																	
	Algorithm: Consider alternative boundary conditions																	
	Algorithm: Characterize error																	
	Algorithm: Characterize Rate of Convergence																	
	Tweak, Debug, Profile, Document																	
	Project Checkpoint Presentation (TBA)																	
	Milestone #2																	
	Finalize Visualization Toolchain (MATLAB wrapper etc)																	
Documentation	Finalize documentation																	
	Milestone #3																	
	Final Presentation																	

Figure 7 Preliminary Gantt chart with relevant milestones.

Milestone 1 (Expected by 03/03/2014)

To have produced set of prototyped functions for segmentation and joint space analysis.

Milestone 2 (Expected by 04/07/2014)

To have finalized the algorithms for segmentation and joint space analysis.

To have thoroughly analyzed the algorithms and documented the results.

Milestone 3 (Expected by 05/09/2014)

To have completed detailed and thorough documentation on the project.

VI. Progress Evaluation

The main source of feedback on progress is going to be meetings with Prof. Siewerdsen, which is set up through the lab Google Calendar page every other Tuesday. Other personnel also attending the meetings are lab technician Tommy Reigel and research fellow Gaurav Thawait, MD. The meetings mainly cover the larger overall study the I-STAR lab is involved with but also gives me an opportunity to present my progress and take suggestions and critiques.

On average, 40 hours a week can be allotted to working on the project.

VII. Dependencies

Dependencies are listed below. They have all been met and are detailed in parentheses:

1. Bi-weekly meeting with mentor (bi-weekly meeting scheduled with Prof. Siewerdsen).
2. CBCT knee volume test data (Two datasets available for algorithm testing and validation).
3. Computing resources.
   i) Up-to-date MATLAB w/ image processing and parallel computing toolboxes (R2013b).
   ii) CUDA-enabled graphics card (NVidia GTX470).
   iii) C++ IDE and compiler (Visual Studio 2008).
   iv) Visualization library (VTK).
4. Access to relevant literature (Lab database & JHU Library Website).

VIII. References

[1] J. R. Giffin, T. M. Vogrin, T. Zantop, S. Woo, and C. D. Harner, "Effects of Increasing Tibial Slope on the Biomechanics of the Knee," Am. J. Sports Med. 32(2): 376-382 (2004).

[2] J. Hashemi, N. Chandrashekar, B. Gill, B. D. Beynnon, J. R. Slauterbeck, R. C. Schutt Jr., H. Mansouri, and E. Dabezies, "The Geometry of the Tibial Plateau and Its Influence on the Biomechanics of the Tibiofemoral Joint," J. Bone and Joint Surg. 90: 2724-2734 (2008).

[3] J. Hashemi, N. Chandrashekar, H. Mansouri, B. Gill, J. R. Slauterbeck, R. C. Schutt Jr., E. Dabezies, and B. D. Beynnon, "Shallow Medial Tibial Plateau and Steep Medial and Lateral Tibial Slopes : New Risk Factors for Anterior Cruciate Ligament Injuries," Am. J. Sports. Med. 38: 54-52 (2010).

[4] S. G. McLean, S. M. Lucey, S. Rohrer, and C. Brandon, "Knee joint anatomy predicts high-risk in vivo dynamic landing knee biomechanics,"Clin. Biomech. (2010) (in press doi:10.1016/j.clinbiomech.2010.06.002).

[5] K. B. Shelburne,H.-J. Kim, W. I. Sterett, and M. G. Pandy, “Effect of Posterior Tibial Slope on Knee Biomechanics during Functional Activity,” Orth. Res. Soc. Feb. 223-231 (2011).

[6] S. J. Shultz and R. J. Schmitz, “Tibial Plateau Geometry Influences Lower Extremity Biomechanics During Landing,” Am. J. Sports Med. 40(9): 2029-2036 (2012).

[7] W. Zbijewski, P. De Jean, P. Prakash, Y. Ding, J. W. Stayman, N. Packard, R. Senn, D. Yang, J. Yorkston, A. Machado, J. A. Carrino, and J. H. Siewerdsen, "A dedicated cone-beam CT system for musculoskeletal extremities imaging: Design, optimization, and initial performance characterization," Med. Phys. 38(8): 4700 - 4713 (2011).

[8] Sokka, T. (2008). Radiographic Scoring in Rheumatoid Arthritis, *66*(2), 166–168.

[9] Hodgson, R. J., O’Connor, P., & Moots, R. (2008). MRI of rheumatoid arthritis image quantitation for the assessment of disease activity, progression and response to therapy. *Rheumatology (Oxford, England)*, *47*(1), 13–21. doi:10.1093/rheumatology/kem250

[10] Kalinosky, B., Sabol, J. M., Piacsek, K., Heckel, B., & Gilat Schmidt, T. (2011). Quantifying the tibiofemoral joint space using x-ray tomosynthesis. *Medical Physics*, *38*(12), 6672–82. doi:10.1118/1.3662891

[11] Yezzi, A. J., & Prince, J. L. (2003). An Eulerian PDE approach for computing tissue thickness. *IEEE Transactions on Medical Imaging*, *22*(10), 1332–9. doi:10.1109/TMI.2003.817775

IX. Acknowledgements

I would like to thank all members of the I-STAR lab for their help and support when I was getting started on this project, especially Dr. Webster Stayman, Dr. Grace Gang, Dr. Adam Wang, Jennifer Xu, Hao Dang, Ali Uneri, Ja Reaungamornrat and Steven Tilley II.